WATER RESOURCES RESEARCH, VOL. 42, W03416, doi:10.1029/2005WR004146, 2006

A fractional dispersion model for overland solute transport

Zhi-Qiang Deng,[1] João L. M. P. de Lima,[2] M. Isabel P. de Lima,[3] and Vijay P. Singh[1]

Received 28 March 2005; revised 28 November 2005; accepted 22 December 2005; published 18 March 2006.

[1] Using the kinematic-wave overland flow equation and a fractional dispersion-advection equation, a process-oriented, physically-based model is developed for overland solute transport. Two scenarios, one consisting of downslope and the other of upslope rainstorm movements, are considered for numerical computations. Under these conditions, the hydrograph displays a long-tailed distribution due to the variation in flow velocity in both time and distance. The solute transport exhibits a complex behavior. Pollutographs are characterized by a steep rising limb, with a peak, and a long, stretched receding limb; whereas the solute concentration distributions feature a rapid receding limb followed by a long stretched rising limb. Downslope moving storms cause much higher peak in both hydrographs and pollutographs than do upslope moving storms. Both hydrographs and the pollutographs predicted by the fractional dispersion model are in good agreement with the data measured experimentally using a soil flume and a moving rainfall simulator.

Citation: Deng, Z.-Q., J. L. M. P. de Lima, M. I. P. de Lima, and V. P. Singh (2006), A fractional dispersion model for overland solute transport, *Water Resour. Res.*, *42*, W03416, doi:10.1029/2005WR004146.

1. Introduction

[2] Overland flow transports solutes which may originate from a variety of sources. Various surface-applied chemical fertilizers, pesticides, and soil-incorporated nutrients in agricultural lands are often transferred from soil to overland flow during rainstorms, resulting in overland solute transport. The overland flow-induced solute transport not only decreases the efficiency of chemical fertilizers applied and thus agricultural productivity, but also poses a potential threat to the quality of water and a serious environmental and health risk. This is the reason that a higher pollutant concentration is observed during flooding [*Singh*, 1997; *Wan and Huang*, 1999].

[3] Some of the many hydrological factors that directly or indirectly affect the overland solute transport may be controlled to minimize environmental pollution and maximize the application efficiency of chemicals. For this purpose a theoretical description of the solute transport process is essential. Consequently, overland flow and accompanying solute transport have been extensively investigated over the past three decades, leading to a large number of overland solute transport models, ranging from simple empirical formulas to comprehensive distributed physically/chemically-based descriptions [*Govindaraju*, 1996; *Abbott and Refsgaard*, 1996; *Singh*, 1997; *Wallach et al.*, 2001; *Singh*, 2002]. The basic equation involved in the models is the mass transport equation: advection-dispersion equation (ADE). For instantaneous release of solute the solution of the ADE leads to Gaussian spatial concentration distributions or Fickian distributions, whereas observed concentrations display a long-tailed distribution or tailing behavior [*van Genuchten and Wierenga*, 1976]. To make the theoretical solution consistent with measurements, a reaction (source/sink) term is often added into the ADE to take into account the mass exchange between overland flow and the active surface layer. The models based on the ADE with the reaction term are usually known as transient storage-release model or dead-zone model [*Hunt*, 1999]. The incorporation of the reaction term makes the solution of ADE exhibit distributions similar to the measured ones to some extent. However, there is lack of theoretical analysis of the soundness of the solution in terms of statistical measures. Such an analysis is essential to determine the applicability of existing models to describe overland solute transport. The basic idea behind the analysis is to compare, using statistical measures, theoretical and measured distributions of solute concentration. If the theoretical statistical measures of the solution of the existing models are close to the measured ones, the existing models may be assumed to be reasonable. Otherwise, a new model is necessary for overland solute transport.

[4] In terms of the long-tailed concentration distributions observed in overland solute transport, variance may be the most important statistical measure of the distribution curves because only the variance is a measure of the spread of the concentration curves among the commonly used statistical measures, such as mean, variance, skewness, and kurtosis. *Hunt* [1999] analyzed temporal variance of the dead-zone model and concluded that temporal variance and peak concentration decay rate of the dead-zone model have behaviors that are similar to the corresponding results for the Fickian model. The variance σ^2 is asymptotically proportional to the longitudinal distance x for a fixed time or to time t for a fixed location for both the Fickian and the dead-zone models, that is, σ^2 is proportional to t. It means that the variance of measurements should also be proportional to t if the existing overland solute transport models

[1]Department of Civil and Environmental Engineering, Louisiana State University, Baton Rouge, Louisiana, USA.
[2]IMAR – Institute of Marine Research, Coimbra Interdisciplinary Centre; Department of Civil Engineering, Faculty of Science and Technology, University of Coimbra, Coimbra, Portugal.
[3]IMAR – Institute of Marine Research, Coimbra Interdisciplinary Centre; Department of Forestry, Agrarian Technical School of Coimbra, Polytechnic Institute of Coimbra, Coimbra, Portugal.

0043-1397/06/2005WR004146$09.00

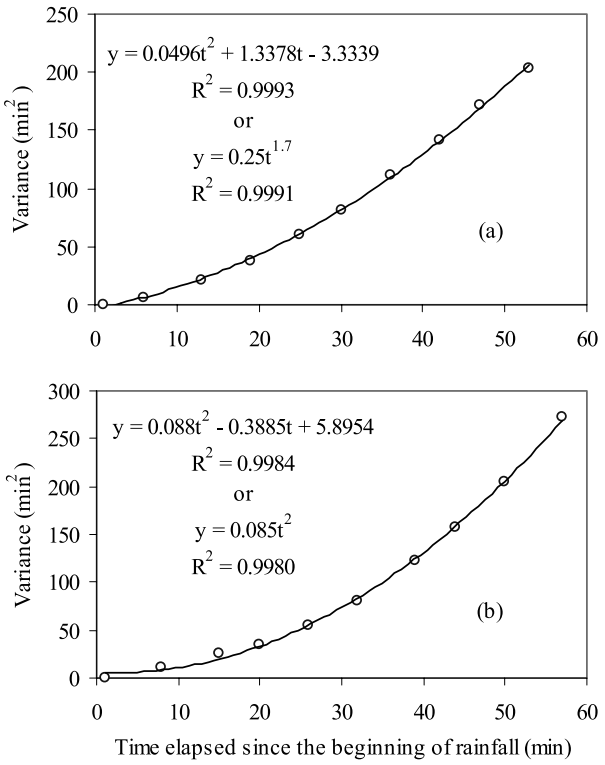

Figure 1. Nonlinear variation of variance of measured solute concentration distributions with time.

are theoretically sound. To that end, observed concentration data of overland solute transport under simulated rainfall [*Hubbard et al.*, 1989a, 1989b] are employed to test the relationship between variance σ^2 and time t. The results of the data analysis show that measured values for the variance are proportional to t^{ξ} in which ξ ranges from 1.70 (R^2 = 0.9991) to 2.00 (R^2 = 0.9980) with a mean of 1.85. Higher R-squared values can be achieved if second-order polynomial trendlines are adopted, as shown in Figures 1a and 1b, where the curves are the second-order polynomial trendlines and y denotes the variance, i.e., $y = \sigma^2$. The variance increases at a rate of $d\sigma^2/dt = \xi t^{(\xi-1)}$. It is apparent that the rate increases nonlinearly to a very large number or even tending to infinity if time tends to be very long, whereas the variance of the Fickian dispersion increases linearly with a much slower rate. The results clearly demonstrate that the measured variance of a plume of the overland solute transport grows much faster than one described by the existing overland solute transport models based on the Fickian dispersion. It implies that a physically sound description of overland solute transport needs either improvement of existing models or a new model.

[5] The second-order polynomial equations of the trendlines shown in Figures 1a and 1b are instructive to the development of a new model for overland solute transport. It is apparent from Figure 1 and the above-mentioned variance analysis that (1) the relationship between variance and time does not simply follow a power law, although approximate power-law relations may be found in some cases; and (2) a polynomial equation with a variable power index can best describe the relation between variance and time. These characteristics of the variance of observed concentration distributions are difficult to predict using existing integer-order models. In fact, the infinite variance is a typical feature of the fractional advection-dispersion equation (FADE) [*Meerschaert et al.*, 1999]. It implies that overland solute transport may be best described by the FADE. This idea motivates the development of a fractional dispersion model for overland solute transport which has not been attempted thus far, to the best of our knowledge. In addition to the inconsistency of the theoretical variance with the measured one, there are also some other problems in existing overland solute transport models.

[6] A multitude of distributions have been reported for the residence time of solutes. *Haggerty et al.* [2002] proposed a power-law residence time distribution for solute dispersion and transport in a 2nd-order mountain stream by introducing a convolution of the hyporheic memory function with solute concentration to the mass balance equation. The method involves parameters, such as the reach volume of the hyporheic zone, the mean residence time in the hyporheic zone, and so on, which are difficult to quantify. It is apparent that in natural media there is a wide spectrum of storage zones with the size ranging from flow width to soil pore diameter. The residence time displays a similar behavior. Moreover, actual distributions of solute concentration or residence time may display a complicated behavior characterized by a polynomial relation between variance and time. The polynomial relation may reduce to a power-law [*Haggerty et al.*, 2002] or an exponential law [*Harvey et al.*, 1996; *Wörman et al.*, 2002] or a lognormal distribution [*Wörman et al.*, 2002], depending on the heterogeneity of the medium. It is therefore not appropriate to attribute the concentration distributions to any specific category of distribution functions, such as power-law.

[7] Another drawback of most existing models is the distinct deviation of the predicted initial concentration distributions from measurements, as shown in Figure 5 of *Wallach et al.* [2001]. In most field and laboratory measurements, as illustrated in Figures 7, 8, and 12 of *Hubbard et al.* [1989a] and in Figures 1 and 6 of *Hubbard et al.* [1989b], the solute concentration declines rapidly from a first flush caused highest initial concentration value, instead of the commonly assumed zero value. Such a significant disagreement is caused by an inappropriate prescription of initial conditions due to the uncertainty of actual initial concentration conditions. For simplicity and convenience of both numerical and analytical solutions, a zero initial concentration is often employed. In terms of practical and environmental concern with overland solute transport, the highest concentration occurring in the initial runoff is most important and hence it should be evaluated as accurately as possible. However, a few existing models can make such a prediction. To that end, it is therefore essential to find a new solute transport equation on the basis of the conventional advective-diffusive equation.

[8] The overall goal of this paper is to develop a fractional dispersion model for overland solute transport as the fractional advection-dispersion equation (FRADE) has been increasingly used in a wide spectrum of scientific areas [*Benson et al.*, 2000a, 2000b; *Berkowitz et al.*, 2002;

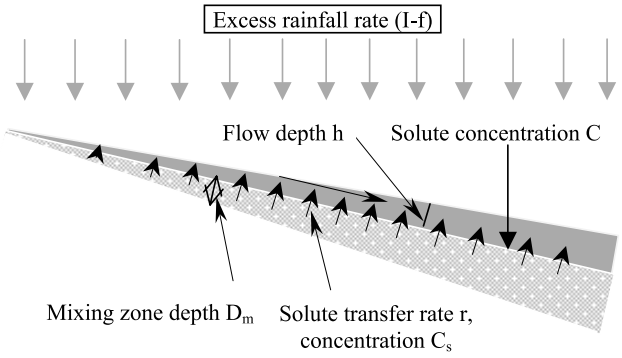

Figure 2. Conceptual model for overland solute transport.

Schumer et al., 2003; *Deng et al.*, 2004] for simulating the long-tailed dispersion caused by heterogeneity of media. The specific objectives are therefore (1) to clarify the processes involved in and the physics responsible for the overland solute transport, (2) to propose an overland flow equation under moving rainstorms, (3) to formulate the fractional dispersion model for overland solute transport, (4) to present numerical solution procedures for the fractional model, and (5) to test the performance of the proposed model.

2. Physical Background of Overland Solute Transport

[9] A conceptual representation of the processes involved in overland flow and solute transport under rainfall is depicted in Figure 2. The soil underlying overland flow is assumed to have a mixing zone or active surface layer through which rainfall infiltrates into the subsurface soil, and the soil transfers solute to surface runoff. This zone is assumed to (1) have a uniform solute concentration C_s; (2) have a thickness $D_m = \varepsilon h$ that is proportional to the depth h of overland flow by a constant ε; and (3) act as a source of chemical supply to overland flow with a mass transfer coefficient of r. The net result of overland solute transport is always a decline in the chemical concentration C_s in the soil and an increase of solute concentration C in the flow, if rainfall has a zero-solute concentration. The main physical processes responsible for overland solute transport include (1) advection of solute due to the Hortonian overland flow formed by excess rainfall; (2) transfer of solute from the active surface layer to the overlying water owing to the concentration gradient between the flowing water layer and the mixing soil layer; (3) dilution or flushing due to rainfall excess ($I - f$), where I is the rainfall intensity and f is the infiltration capacity of soil; and (4) solute dispersion due to velocity and concentration gradients in the heterogeneous medium. It is important to have a clear understanding of heterogeneity of media.

[10] For overland flow and solute transport, the heterogeneity of media is embodied in two ways: surface heterogeneity and volume heterogeneity. The volume heterogeneity refers to the heterogeneously aggregated nature of the active surface layer. Soils are aggregated media comprised of soil particles and interconnected soil pores with diameters ranging from large to small, or from macropores to mesopores and further to micropores. Solutes in micropores within soil aggregates are transported to macropores by diffusion, while they are transported by advection with moving water in soil macropores. The release process of solutes in micropores will thus take a much longer time than that in macropores, because the diffusion pathway is much longer than the advection pathway. This results in breakthrough curves with more and longer tailing. *van Genuchten and Wierenga* [1976] described in detail the mass transfer in porous media. The surface heterogeneity represents irregularity and roughness of the soil surface, such as surface depressions, microtopography, undulations caused by heterogeneous erosion, among others. Solute transport processes are generally accompanied by heterogeneous soil erosion. No matter how homogeneous the initial soil surface is, the erosion process frequently occurs in a heterogeneous manner. It implies that the soil surface is not eroded uniformly. Some rills may be formed during the erosion process, causing heterogeneous wash-off of solutes on the soil surface. Such heterogeneous erosion causes a hierarchical and delayed release of solutes. The surface heterogeneity also constitutes fractal roughness and thus a series of storage – release zones of solutes. In the concentration rising stage solutes may be trapped in the storage zones and then gradually released in the concentration receding stage, elongating the tail part of the concentration curves. The surface heterogeneity may exist on the surface of relatively homogeneous soils and even on the surface of urban pavements. Based on such a consideration of heterogeneity, almost all natural watersheds are heterogeneous. The observed tailing in the breakthrough curves of concentration is caused by the combined effect of surface heterogeneity and volume heterogeneity. The relative importance of surface heterogeneity and volume heterogeneity varies with both the location and the time and is therefore of complex and dynamic nature. If the surface is very rough, surface heterogeneity may play a dominant role. Otherwise, volume heterogeneity may control the tailing behavior. Based on the above conceptualization for model construction, the mechanisms and processes of overland solute transport can be described by a new mathematical model, which is discussed in what follows.

3. Fractional Dispersion Model for Overland Solute Transport

3.1. Water Flow Equations Under Moving Rainstorms

[11] Overland flow or the motion of a water-wave propagating on an initially dry soil surface with a steep uniform slope is commonly described by the one-dimensional Saint-Venant shallow-water equations, which are an approximation of the laws of conservation of mass and momentum of the shallow water flowing longitudinally and infiltrating vertically [*Singh*, 1996]. A commonly accepted approximation of the St Venant equations for overland flow is the kinematic wave equation which can be expressed as

$$\frac{\partial h}{\partial t} + \frac{\partial (uh)}{\partial x} = I - f \tag{1a}$$

with

$$u = \alpha h^{m-1} \quad \text{or} \quad Q = \alpha W h^m$$
$$\left(\alpha = \sqrt{S}/n_m \ \text{ and } \ \mathrm{m} = 5/3 \text{ for turbulent flow}\right) \tag{1b}$$

where Q is the flow discharge; W is the width of the land; $h = h(x, t)$ is the depth of overland flow; $u = u(x, t)$ is the velocity of the flow; $I = I(x, t)$ is the rainfall intensity and it depends on the location and time for moving rainstorms; $f = f(x, t)$ is the infiltration rate; t is time; x is distance along the flow direction; m is an exponent; and α is the kinematic-wave resistance parameter; n_m denotes Manning's roughness coefficient; and S represents the longitudinal slope of the soil surface. Owing to the impact of rainfall drops, overland flow is assumed to be turbulent and then parameters m and α can be determined from Manning's formula.

[12] Solution of the kinematic wave equations (1a) and (1b) requires only an upstream boundary condition. Therefore the initial and boundary conditions imposed on equation (1a) can be defined as:

$$h(x, 0) = 0, \quad 0 \le x < L \tag{1c}$$

$$h(0, t) = 0, \quad 0 \le t < \infty \tag{1d}$$

The problem of overland flow is reduced to the solution of equation (1a) subject to equations (1c) and (1d).

3.2. Fractional Dispersion Equations of Solute Transport

[13] Solute transport in flowing fluids is often described by an advection-dispersion equation with a transient storage-release term or dead-zone term [*van Genuchten and Wierenga*, 1976; *Hunt*, 1999]. In principle, the same equation can be employed to describe overland solute transport. Actually, the solute transport equation for overland flow can be derived easily following the similar approach used in Appendix B from the mass conservation principle and the Reynolds transport theorem. The equation can be expressed in a conservative form in terms of the solute flux as:

$$\frac{\partial(Ch)}{\partial t} + \frac{\partial(Cuh)}{\partial x} = \frac{\partial}{\partial x}(-hJ) + rD_m(\mathrm{C_s} - C) \tag{2a}$$

where C stands for the cross-sectionally averaged solute concentration or the mass of solutes per unit volume of runoff with a dimension of [M/L^3]; C_s represents the solute concentration in the mixing soil zone; r is a mass transfer coefficient with a dimension of [1/T]; D_m is the mixing zone thickness which is proportional to flow depth; and J denotes the flux of dispersion in heterogeneous media. A proper definition of the flux J is important to the application of the equation. Traditionally, mass transport media are assumed to be isotropic and the flux is expressed as $J = -K\partial C/\partial x$ [*Fischer et al.*, 1979]. However, natural media, such as soil, rivers, etc., for solute transport are rarely isotropic as mentioned earlier. To describe the dispersion process in anisotropic media, *Chaves* [1998] and *Meerschaert et al.* [1999] proposed a general flux law of molecular diffusion based on the revision of Fick's diffusion law. On the basis of the general flux law and the analogy of turbulent diffusion and shear flow dispersion with the molecular diffusion, a more general law of solute dispersion in the overland flow can be defined as:

$$J = -D_{mo}\left[s_m \frac{\partial^{F-1}C}{\partial x^{F-1}} - (1 - s_m)\frac{\partial^{F-1}C}{\partial x^{F-1}}\right] - D_t\left[s_t \frac{\partial^{F-1}C}{\partial x^{F-1}} - (1 - s_t)\frac{\partial^{F-1}C}{\partial x^{F-1}}\right] - K\frac{\partial^{F-1}C}{\partial x^{F-1}} \tag{2b}$$

where D_t is the turbulent diffusion coefficient; K is the longitudinal dispersion coefficient; F is a fractional differential order; s_m and s_t describe the skewness of the transport process [*Chaves*, 1998; *Benson et al.*, 2000b]. The first term on the right hand-side (RHS) of equation (2b) represents the solute flux produced by the molecular diffusion; the second term on the RHS stands for the solute flux produced by the turbulent diffusion; and the third term denotes the solute flux produced by the shear flow dispersion. The first two terms are much smaller than the last term, because the molecular and turbulent diffusion coefficients D_{mo} and D_t are much smaller than the shear flow dispersion coefficient K [*McCutcheon*, 1989]. It should be pointed out that in principle the last term on the RHS of equation (2b) should also be expressed as a linear combination of the Reimann-Liouville operator (the derivative of a function from $-\infty$ to x) and the Weyl fractional derivative (the derivative from x to ∞) [*Benson et al.*, 2000b; *Schumer et al.*, 2001]. Physically, the Reimann-Liouville fractional derivative, characterized by a long range-dependence or memory, describes the solute flux at any point affected by the solutes released from all upstream points where solutes may be stored transiently and released gradually. The delayed release of solutes produces an additional flux or concentration at the downstream point. The Weyl fractional derivative was introduced to the fractional advection-diffusion equation by simulating the continuous time random walks (CTRW) of molecules [*Meerschaert et al.*, 1999] in the upstream direction and thus the Weyl fractional derivative represents the diffusion contribution of any downstream points to a specified upstream location due to molecular diffusion. For solute dispersion and transport in overland flow and rivers, the contribution of molecular diffusion or the influence of the Weyl fractional derivative is negligible as compared to the dispersion contribution represented by the Reimann-Liouville derivative. Therefore equation (2b) can be simplified by neglecting the first two terms as

$$J = -K\frac{\partial^{F-1}C}{\partial x^{F-1}} \tag{2c}$$

The minus sign in equation (2c) means that dispersion is down the concentration gradient. The longitudinal dispersion coefficient K carries the dimension of [L^F/s] and it is a variable in principle. A variable dispersion coefficient has been used in some scale-dependent dispersion models [*Wheatcraft and Tyler*, 1988; *Hunt*, 1999], but there are no theoretical methods available for estimation of the variable K. The dispersion coefficient K for overland solute transport can be evaluated during model calibration by

means of laboratory experiments. The advantage of using equation (2c) to describe the flux law of dispersion in heterogeneous media like the soil is the separation of the scale effect from the values of the dispersion coefficient. The scale effects are reflected by the order of the fractional derivative, and the dispersion coefficient K needs to be found for only one scale. Substituting equation (2c) into equation (2a) and rearranging the terms yields

$$C\left(\frac{\partial h}{\partial t}+\frac{\partial (uh)}{\partial x}\right)+h\left(\frac{\partial C}{\partial t}+u\frac{\partial C}{\partial x}\right)=Kh\frac{\partial^F C}{\partial x^F} + K\frac{\partial h}{\partial x}\frac{\partial^{F-1} C}{\partial x^{F-1}}+rD_m(\mathrm{C_s}-C) \quad (3)$$

The fractional differential order F, called fractor, physically reflects the heterogeneity of the soil medium in which solute is transported in a lumped fashion. For isotropic media, $F = 2$. The more heterogeneous the medium is, the smaller the fractor F is than the integer constant of 2. A decrease in F will lead to an increase in the mean travelling time of solute. It means that the decrease in F causes an increase in the resistance of the medium to solute dispersion and transport, resulting in an increased travelling time of the solute or a long-tailed dispersion. Therefore the fractional differential order F is also a measure of the strength of the persistence in the dispersion process.

[14] A comparison between the finite-difference approximation of the integer-order derivative and the numerical approximation of the fractional derivative may be helpful for understanding the physical meaning of the fractional derivative and the fractional dispersion term involved in equation (3). In the conventional numerical methods the integer order derivatives are generally approximated by a few neighboring grid points whose values are known. However, the fractional derivative is a convolution that depends on all the values of the points in the computational domain with a different ''memory.'' Therefore fractional derivatives are commonly approximated by a series [*Oldham and Spanier*, 1974; *Podlubny*, 1999; *Deng et al.*, 2004]. Based on the definition of fractional derivatives, the fractional dispersion term physically represents the long-tailed dispersion process caused by the hierarchical release of the solute stored in the dead-zones in the soil due to the surface heterogeneity and the volume heterogeneity mentioned previously. The long-tailed dispersion process is characterized by concentration versus time curves with a growing nonlinear variance. Although the incorporation of a dead-zone term in the advection-dispersion equation can improve the performance of the dead-zone models, they are essentially the same as the Fickian dispersion model in terms of the variance [*Hunt*, 1999]. The fractional derivatives-based mass transport equation, the fractional advection-dispersion equation (FADE), can yield a concentration curve with a growing nonlinear variance. This is why the FADE is increasingly used to simulate the long-tailed dispersion process of solute in groundwater [*Benson et al.*, 2000a, 2000b; *Schumer et al.*, 2003; *Zhou and Selim*, 2003]. Due to the non-local or long-range dependence feature, the fractional derivatives are particularly suitable to the description of mass dispersion and transport in heterogeneous media.

[15] According to the results obtained for natural rivers, including wide and shallow rivers with width-depth ratios greater than 100 [*Deng et al.*, 2004], fractor F varies in the range from 1.4 to 2.0 around the most frequently occurring value of $F = 1.65$. For modelling overland solute transport in ungauged watersheds, the value of fractor F can be estimated with reference to the range of $F = 1.4–2.0$. A value of $F = 1.65$ is recommended to the watersheds with moderate heterogeneity. In terms of the kinematic wave approximation $\partial h/\partial x = 0$, substituting equation (1a) into equation (3) and dividing both sides of equation (3) by the flow depth h gives

$$\frac{\partial C}{\partial t}+u\frac{\partial C}{\partial x}=K\frac{\partial^F C}{\partial x^F}+r\varepsilon(\mathrm{C_s}-C)-\frac{(I-f)}{h}C \quad (4a)$$

where $\varepsilon = D_m/h$ is introduced. Equation (4a) involves four processes of solute transport. The second term on the left-hand-side (LHS) of equation (4a) denotes advection caused by overland flow. The fractional-order derivative term on the right hand side (RHS) of the equation represents the contribution of dispersion in a heterogeneous medium like a watershed. The second term on the RHS reflects the transfer of solute from the active surface layer of the soil to the overlying water, and the last term of equation (4a) stands for the flushing resulting from the rainfall excess. In theory, equation (4a) may be employed to predict distributions of concentration C, that are usually characterized temporally by a rising limb followed by a receding limb, by assuming a zero initial concentration C_0 [*Abbott and Refsgaard*, 1996; *Wallach et al.*, 2001]. Unfortunately, for the overland solute transport measured concentration curves often exhibit the first flush phenomenon: a rapidly falling limb followed by a prolonged receding limb. The significant disagreement between the theoretically simulated and actually measured concentration distributions is attributed to the inappropriate definition of initial and boundary conditions of the concentration $C(x, t)$ due to the uncertainty of the initial values of the concentration. However, the initial value of solute transport rate or solute discharge has a fixed value of zero. Therefore, to avoid the use of uncertain initial concentration, equation (4a) can be transformed into a transport rate equation. To that end, replacing C by CQ_f/Q_f and C_s by C_sQ_f/Q_f and then rearrangement of terms leads to

$$\frac{\partial \overline{C}}{\partial t}+u\frac{\partial \overline{C}}{\partial x}+Q_f\left[\left(\frac{\partial (1/Q_f)}{\partial t}+u\frac{\partial (1/Q_f)}{\partial x}\right)-K\frac{\partial^F (1/Q_f)}{\partial x^F}\right]\overline{C} = K\frac{\partial^F \overline{C}}{\partial x^F}+r\varepsilon(\overline{C}_\mathrm{s}-\overline{C})-\frac{(I-f)}{h}\overline{C} \quad (4b)$$

where Q_f is the flow discharge, $\overline{C} = CQ_f$ and $\overline{C}_s = C_sQ_f$ are introduced and are termed the transport rate of solute in the flow and the transport rate of solute from the soil to the flow, respectively. For simplicity the third term on the LHS of equation (4b) without $\overline{C}$ is assumed as $\overline{Q}_f$. Rearranging the terms and using the kinematic wave approximation $\partial h/\partial x = 0$ and equations (1a) and (1b) leads to

$$\overline{Q}_f=Q_f\left[\left(\frac{\partial (1/Q_f)}{\partial t}+u\frac{\partial (1/Q_f)}{\partial x}\right)-K\frac{\partial^F (1/Q_f)}{\partial x^F}\right]\approx -\frac{mq}{h} \quad (4c)$$

in which $q = I - f$ and noting that the dispersion related term is much smaller than the term $d(1/Q_f)/dt$. Substituting equation (4c) into equation (4b) and introducing $E = r\varepsilon$ and $Y = q/h + \overline{Q}_f = (1 - m)q/h$ yields

$$\frac{\partial \overline{C}}{\partial t} + u\frac{\partial \overline{C}}{\partial x} = K\frac{\partial^F \overline{C}}{\partial x^F} + E\left(\overline{C}_s - \overline{C}\right) - Y\overline{C} \tag{4d}$$

[16] Solutes are generally washed off gradually rather than instantaneously. Based on the mass conservation principle and the Reynolds transport theorem, the decay of solutes in the mixing zone caused by the transfer of solutes from the mixing-zone to the overlying runoff can be modeled by the following exponential law with a decay coefficient μ carrying a dimension of [1/T] (see Appendix B):

$$\overline{C}_s = \overline{C}_0 \exp(-\mu t) \tag{4e}$$

Equation (4e) shows the wash-off process of diffuse sources, since the result of overland solute transport is always the decline of solute content in the soil in the absence of production or creation. Initial and boundary conditions are

$$\overline{C}(x,0) = 0, \quad \overline{C}_s(x,0) = \overline{C}_0(x), \quad 0 \le x \le L \tag{4f}$$

$$\overline{C}(0,t) = 0, \qquad 0 \le t < \infty \tag{4g}$$

[17] Due to the full consideration of the main processes and physics of solute transport involved in overland flow, the new model is process-oriented and physically-based. Moreover, equation (4) recovers the integer-order advection-dispersion equation with reaction terms when $F = 2$. It can therefore be employed as a generalized model for overland flow and solute transport in terms of the fractional differential order F.

4. Numerical Solution for Flow and Solute Transport Equations

[18] The objective is to solve equation (4d) for the transport rate $\overline{C}$ of solute at the outlet. To that end, the flow depth h must first be solved from equation (1) and then the value of $\overline{C}$ at each grid point must be determined.

4.1. Numerical Scheme for Kinematic Wave Equation

[19] Several numerical techniques are available for the solution of the kinematic wave equation. One of the most popular second-order finite-difference schemes for overland flow is the Lax-Wendroff (LW) scheme [*Woolhiser*, 1975; *Singh*, 1996]. The essence of the LW scheme lies in the Taylor series expansion of the dependent variable h by ignoring the terms whose order is higher than two, i.e.,

$$h(x, t + \Delta t) = h(x,t) + \Delta t\frac{\partial h}{\partial t} + \frac{(\Delta t)^2}{2!}\frac{\partial^2 h}{\partial t^2} \tag{5}$$

where $\partial h/\partial t$ is obtained from equation (1a) as

$$\frac{\partial h}{\partial t} = q(t) - m\alpha h^{m-1}\frac{\partial h}{\partial x} \qquad (q = I - f) \tag{6}$$

The second-order derivative can be found by differentiating equation (6) as

$$\frac{\partial^2 h}{\partial t^2} = \frac{\partial q}{\partial t} - \alpha\frac{\partial}{\partial x}\left[mh^{m-1}\left(q - m\alpha h^{m-1}\frac{\partial h}{\partial x}\right)\right] \tag{7}$$

It should be noted that the exchange of differential order is carried out in the derivation of equation (7) based on the continuity of the second derivatives of h^m [*Tuma and Walsh*, 1998]. Substituting equations (6) and (7) into equation (5) and applying the FTCS (Forward Time and Centered Space) differencing scheme yield the following explicit second-order finite-difference solution of the kinematic wave equation (details of the derivation can be found in the work of *Singh* [1996]):

$$\begin{aligned} h_j^{i+1} = h_j^i + \Delta t\Bigg(q_j^i - m\alpha\frac{h_{j+1}^{i^{m-1}} + h_{j-1}^{i^{m-1}}}{2}\frac{h_{j+1}^i - h_{j-1}^i}{2\Delta x}\Bigg) \\ + \frac{(\Delta t)^2}{2}\frac{q_j^{i+1} - q_j^i}{\Delta t} - m\alpha\frac{(\Delta t)^2}{2}\Bigg[\frac{h_{j+1}^{i^{m-1}} + h_j^{i^{m-1}}}{2}\Bigg(\frac{q_{j+1}^i + q_j^i}{2} \\ - m\alpha\frac{h_{j+1}^{i^{m-1}} + h_j^{i^{m-1}}}{2}\frac{h_{j+1}^i - h_j^i}{\Delta x}\Bigg) \\ - \frac{h_j^{i^{m-1}} + h_{j-1}^{i^{m-1}}}{2}\Bigg(\frac{q_j^i + q_{j-1}^i}{2} - m\alpha\frac{h_j^{i^{m-1}} + h_{j-1}^{i^{m-1}}}{2}\frac{h_j^i - h_{j-1}^i}{\Delta x}\Bigg)\Bigg]\Bigg/\Delta x \end{aligned} \tag{8a}$$

where superscript i denotes the time step and subscript j stands for the distance step; and Δx and Δt refer to the distance and time step lengths, respectively. For the downstream boundary point, equation (8a) is no longer valid and a first-order scheme is employed as

$$h_j^{i+1} = h_j^i + \Delta t\left(q_j^i - m\alpha\frac{h_j^{i^{m-1}} + h_{j-1}^{i^{m-1}}}{2}\frac{h_j^i - h_{j-1}^i}{\Delta x}\right) \tag{8b}$$

To ensure the numerical stability of the LW scheme, the distance step Δx and time step Δt should be chosen according to the Courant condition:

$$\frac{\Delta t}{\Delta x} \le \frac{1}{\alpha\, mh^{m-1}} \tag{9}$$

Equation (8) should be coupled with the solute transport equation for each time step.

4.2. Numerical Solution of Fractional Dispersion-Advection-Reaction Equation

[20] A variety of numerical schemes are available for approximation of the classical advection-dispersion equation [*Holly and Usseglio-Polatera*, 1984; *Karpik and Crockett*, 1997]. However, a few methods are available for solving fractional partial differential equations (PDEs). Recently, *Deng et al.* [2004] presented a new numerical scheme, called F.3 central finite-difference scheme, for the solution of fractional PDEs. The F.3 scheme is composed of a series expression since the fractional derivative is a convolution that depends on all the values of the points in the computational domain with a long but different "memory."

[21] The split-operator method proposed by *Holly and Preissmann* [1977] and developed by *Holly and Usseglio-Polatera* [1984] is widely used as an efficient technique for the solution of the advection-dispersion equation. In terms of the split-operator, the advection-dispersion equation is decomposed into the hyperbolic (pure advection) and the parabolic (pure dispersion with sink and source terms) partial differential equations. The two sub-equations are then solved separately in two or three consecutive fractional steps by the corresponding numerical approaches that best fit the features of each PDE for one time step. Based on the split-operator algorithm it is commonly assumed that the pure advection process and the pure dispersion process alternate with time: the advection process occurs in the first sub-time step, the dispersion takes place in the second sub-time step, and the reaction is considered in the final sub-time step for one time step [*Holly and Preissmann*, 1977]. Therefore solution of equation (4d) in one time step is the combination of solutions in the sub-steps of advection, dispersion and reaction (flushing in this paper). The most popular split-operator method involves the Semi-Lagrangian (SL) approach [*Holly and Preissmann*, 1977; *Karpik and Crockett*, 1997] in which the advection part is resolved by tracking particles representing parcels of water and solutes in the Lagrangian frame of reference, whereas the dispersion part is solved by using an appropriate finite-difference method in the Eulerian frame of reference. SL tries to combine the grid-point or regular resolution nature of the Eulerian approaches with the enhanced stability of the Lagrangian schemes. The fundamental principle of the split-operator method is embodied in the advection, dispersion, and flushing sub-steps.

4.2.1. Solution of Advection Equation: Semi-Lagrangian Approach

[22] The pure advection process in equation (4d) can be simulated by the following hyperbolic sub-equation:

$$\frac{\partial \overline{C}}{\partial t} + u\frac{\partial \overline{C}}{\partial x} = 0, \quad t \in \left(t^n, t^{n+1/3}\right) \tag{10}$$

Equation (10) is essentially the total derivative of the transport rate $\overline{C}$, i.e.,

$$\frac{d\overline{C}}{dt} = 0 \tag{11}$$

along the scalar trajectory or the characteristic line defined by

$$\frac{dx}{dt} = u(x,t) \tag{12}$$

Integrating equation (11) along the characteristic line of equation (12) and using the explicit second-order Runge-Kutta (midpoint) method [*Press et al.*, 1988] give

$$\overline{C}_a^{t+\Delta t/3} = \overline{C}_d^{t} \tag{13a}$$

$$\begin{aligned} x_d &= x_a + \int_{t+\Delta t/3}^{t} u(x,t)dt = x_a - \int_{t}^{t+\Delta t/3} u(x,t)dt \\ &= x_a - \frac{\Delta t}{3} u\left(\frac{x_d + x_a}{2}, t_{n+1/6}\right) \end{aligned} \tag{13b}$$

where subscripts a and d denote the arrival (at time t+ Δt/3) and departure (at time t) points of the fluid parcel considered. Equation (13a) signifies that the transport rate $\overline{C}$ is maintained along the trajectory in the absence of sources/sinks and dispersion. It means that the transport rate of each grid point x_a (the "arrival" point) at the new time level t+ Δt/3 can be determined via the transport rate of its departure point x_d at the previous time level t. In principle, the transport rate of all grid points at time level t should be known. However, the departure point x_d typically will not fall on a grid point and thus the location and transport rate of the departure point x_d must first be determined. Therefore, in the semi-Lagrangian formulation, two distinct steps are required: for each grid point x_a, one first needs to integrate equation (12) backward in time to determine the location of the departure point x_d of that same fluid element at time t. The second step consists of interpolating the transport rate $\overline{C}$ of the departure point x_d using the known values of two neighboring grid points and finally replacing that value at x_a according to equation (13a). Numerous interpolation methods exist [*Press et al.*, 1988]. Cubic splines are the most popular interpolating functions. These smooth functions do not have a significant oscillatory behavior that is characteristic of high-degree polynomial interpolators, such as the Lagrangian Interpolator, Hermite Interpolator, etc. Moreover, cubic splines have the lowest interpolation error of all fourth-order interpolating polynomials. Therefore the commonly used natural cubic splines were adopted to perform the required interpolation. The "natural" implies that the second derivative of the spline function is set to zero at the endpoints, since this provides a boundary condition that completes the system of n-2 equations, leading to a simple tridiagonal system which can be solved easily.

4.2.2. Solution of Fractional Dispersion-Transfer Equation: F.3 Scheme

[23] The dispersion and transfer processes in equation (4d) can be simulated by the following sub-equation in conjunction with equation (4e):

$$\frac{\partial \overline{C}}{\partial t} = K\frac{\partial^F \overline{C}}{\partial x^F} + E\left(\overline{C}_s - \overline{C}\right), \quad t \in \left(t^{n+1/3},\ t^{n+2/3}\right) \tag{14}$$

Utilizing the forward time scheme and the F.3 central finite-difference scheme [*Deng et al.*, 2004], equation (14) can be discretized. Then, having all the known quantities appear on the RHS and all the unknown quantities appear on the LHS yields (see Appendix A) one obtains:

$$O\overline{C}_{j-1}^{n+2/3} + P\overline{C}_{j}^{n+2/3} + Q\overline{C}_{j+1}^{n+2/3} = R^{n+1/3} \tag{15a}$$

where

$$\begin{aligned} &O = -w_2^F\varphi\lambda, \quad P = 1 + \beta + \varphi\lambda F, \quad Q = -\varphi\lambda, \\ &R^{n+1/3} = \varphi(1-\lambda)\overline{C}_{j+1}^{n+1/3} + [1 - \beta - F\varphi(1-\lambda)]\overline{C}_{j}^{n+1/3} \\ &\qquad + w_2^F\varphi(1-\lambda)\overline{C}_{j-1}^{n+1/3} + \gamma\beta\overline{C}_{sj}^{n+1/3} \\ &\qquad + \varphi\sum_{l=0}^{n}\sum_{i=j+2}^{N} w_k^F\overline{C}_{i}^{l+1/3} \end{aligned} \tag{15b}$$

For $j = 0$ to N, equation (15a) can be written as a tridiagonal matrix, a system of simultaneous linear algebraic equations.

Therefore the equations can be solved efficiently using the Thomas Algorithm and the initial and boundary conditions in equations (4f) and (4g). It is assumed that the values of transport rate at points $j - 1$ and j are zero for $j = 0$ and the values of transport rate at point j+1 are identical to that of point j for $j = N$. Then, the value of $\overline{C}$ at each grid point at the time level $(n + 2/3)\Delta t$ is found. It should be noted that parameter Y is a variable instead of a constant like E. The flushing term with Y should therefore be solved independently.

4.2.3. Solution of Flushing Equation: Integration-Based Analytical Method

[24] The rainfall flushing process in equation (4d) can be simulated by the following sub-equation

$$\frac{\partial \overline{C}}{\partial t} = -Y\overline{C}, \quad t \in \left(t^{n+2/3}, t^{n+1}\right) \tag{16}$$

Integrating equation (16) and using the trapezoidal rule of numerical integration yield

$$\begin{aligned} \overline{C}_j^{n+1} &= \overline{C}_j^{n+2/3} \exp\left(-\int_{(n+2/3)\Delta t}^{(n+1)\Delta t} Y dt\right) \\ &\approx \overline{C}_j^{n+2/3} \exp\left[-\frac{\Delta t}{6}\left(Y_j^{n+2/3} + Y_j^{n+1}\right)\right] \end{aligned} \tag{17}$$

where $C_j^{n+2/3}$ is known from equation (15) and Y_j^{n+1} is calculated by means of equation (8). The value of $Y_j^{n+2/3}$ is assumed to be identical to that of Y_j^n. Parameters K, E, and Y should be taken as zero if $u = 0$. More detailed information about the numerical solution for fractional advection-dispersion equation can be found in the work of *Deng et al.* [2004].

5. Description of Laboratory Experiments: Materials and Methods

[25] The performance of the fractional dispersion model described above was tested by comparing the output of the model with results from a series of laboratory experiments conducted in a soil flume using a movable sprinkling-type rainfall simulator. The aim of the laboratory setup was to simulate short-duration natural storms induced by steady one-directional winds.

5.1. Experimental Setup

5.1.1. Characteristics of the Flume and Soil

[26] The soil flume was constructed with metal sheets and had the following dimensions: 2.0 m length × 0.1 m width × 0.12 m height. No buffer zone was used around the plot in order to compensate for water and sediments ejected outside the flume. Surface runoff and free percolation water were collected at the end of the flume. The flume bed had a slope of 10%. The soil material used in the laboratory experiments was mainly composed of quartz, feldspars, quartzite, muscovite and clay minerals. It consisted of 11% clay, 10% silt and 79% sand. This terrigenous sedimentary material soil was collected from the right bank of the Mondego River in the city of Coimbra, Portugal.

[27] The original soil material was submitted to a standard procedure involving pre-sieving for removing coarse rock and organic debris, prior to being uniformly spread in the flume. To obtain a flat surface, a sharp, straight-edged blade that could ride on the top edge of the sidewalls of the flume was used to remove excess soil. The blade was adjusted such that the soil level in the flume equalled the retaining bar at the bottom end of the flume. Afterwards, the soil was gently tapped with a wooden block, aiming to attain a uniform bulk density of approximately 1100 kg/m^3. The resulting soil surface was smooth, and contained no rough elements, such as micro-topographic protuberances, stones or plant stems. The soil had a uniform thickness of 0.1 m.

[28] Standard laboratory permeability tests yielded a saturated hydraulic conductivity of $K_s = 5.7 \times 10^{-5}$ m/s with a standard deviation of 1.8×10^{-5} m/s, for 10 replicates. The saturated soil water content was 39%. The samples tested were obtained following exactly the same procedure as that used to fill the flume, and had the same bulk density.

5.1.2. Characteristics of the Rainfall Simulator

[29] The basic components of the rainfall simulator were three equally-spaced downwards-directed full-cone nozzles, a wheeled support structure holding the nozzles, and the connections to the water supply and the pump. The distance between nozzles was 0.95 m. The nozzles were 2.2 m above the geometric centre of the soil surface. The working pressure on the nozzles was kept constant at 50 kPa. The water used in the rainfall simulation was tap water. Its characteristics are described by *de Lima et al.* [2002]. The simulated rainfall consisted of small drops with an approximately 1.5 mm median diameter.

5.2. Experimental Procedure

[30] The laboratory work consisted of simulating rainstorms moving upstream and downstream, with a speed of 0.18 m/s, over the soil surface, to study overland flow and associated solute transport. The experimental data is summarized in Table 1. The storm movement was simulated by wheeling the nozzle support structure, back and forth, over the flume at a constant speed. Notice that this is a windless rainfall, although the storms move. Because of the wind-free laboratory conditions, there was no interaction of the simulated raindrops and sediments with wind (e.g., wind drag effects). Each experiment was formed by a sequence of three consecutive simulated rainfall events, moving in a given direction (i.e., moving in the downslope or in the upslope direction). For a given storm a constant spatial intensity pattern was maintained for the entire duration of simulation (time required for the storm to cross the plane). The total time, the rainfall is felt on the surface (duration of the storm) from the instant the rainfall enters (at $x = 0$) until it leaves (at $x = L$) the surface, is: $D = (L + L_S)/V_S$, in which D is the duration of the storm (s), L is the length of the flume (m), L_s is the length of storm (m), and V_S is the speed of the storm (m/s). In this study, $D = 40$ s.

[31] The distribution of rainfall intensity supplied by the rainfall simulator (static) on a horizontal surface is presented in Figure 3. To measure the distribution, rectangular containers with dimensions of 0.11 m × 0.11 m × 0.05 m were distributed in line with a distance interval of 0.115 m in a horizontal flume. The volume of rainfall collected in the containers was measured and converted to rainfall depth per minute. The average storm intensity was 3.24 mm/min and the length of the storm (length of water application to the soil surface along the slope) was 5.3 m. The rainfall

Table 1. Summary of Experimental Data

	Dimensions					
	Length	Width	Height			Slope
Flume	2.0 m	0.1 m	0.12 m			10%
			Soil Composition			
	Bulk Density	Hydraulic Conductivity	Clay	Silt	Sand	Saturated Water Content
Soil	1100 kg/m^3	5.7×10^{-5} m/s	11%	10%	79%	39%
	Length (Along the Slope)	Average Intensity	Storm Velocity (Downstream and Upstream, Along the Slope)			
Simulated Rainfall	5.3 m	3.24 mm/min	0.18 m/s			
	Type	Weight	Application			
Solute	salt (sodium chloride)	0.025 kg (grain)	uniformly distributed			

intensity was assumed constant along the width of the flume. The shape of the rainfall hyetograph at each point of the flume is identical to the shape of the spatial rainfall distribution presented in Figure 3, considering however a different time scale, since it is a histogram composed of pulses (each pulse has a different value of lateral inflow and duration). To simulate the presence of surface pollutants, 25 g of granular salt (sodium chloride) was applied uniformly on the soil surface. After applying the salt, the soil was subjected to a series of simulated rainfall events, all moving in the same direction, which induced overland flow and solute transport.

[32] Before starting experimental runs, the soil was wetted up to field capacity. The consecutive rainfall events were generated at regular time intervals (about 15 minutes) to attain approximately the same initial moisture conditions in the surface layer of the soil. Volumetric soil water content was approximately 20% (determined by Time-Domain-Reflectometer measurements) just before the start of the storm events.

[33] Overland flow, sediment transport and solute transport caused by each rainfall event were measured by collecting samples every 10 seconds in metal containers placed at the downstream end of the soil flume. The measurement starting-time in each storm event corresponded to the initiation of overland flow at the outlet of the flume. The simulated rainstorms were conducted under free-draining conditions. The salt transported by overland flow was estimated using a calibrated portable conductivity-meter.

6. Application of the Fractional Dispersion Model and Discussion of Results

[34] To test the applicability of the proposed model, the kinematic-wave flow equation and fractional dispersion-

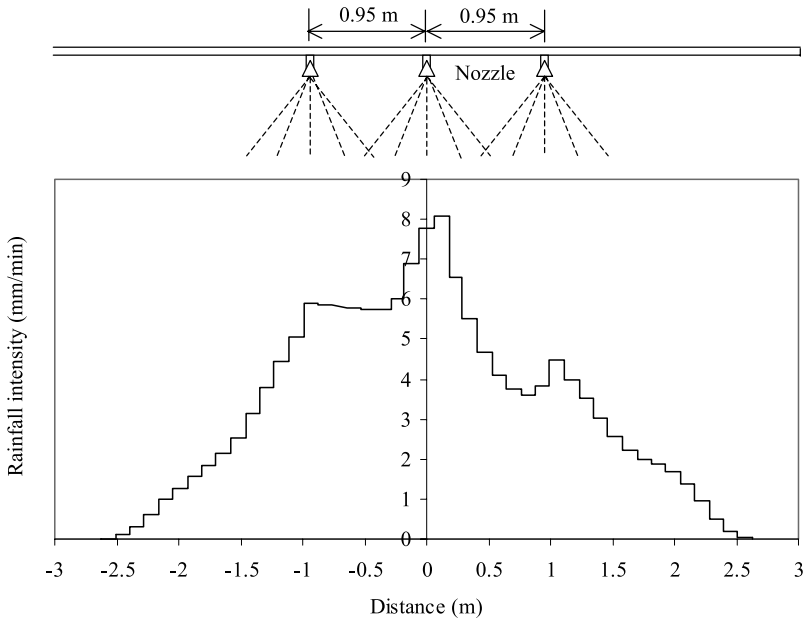

Figure 3. Rainfall under three nozzles.

Table 2. Parameters Used in the Fractional Dispersion Model

	Parameter				
Storm Direction	F	K (m^F/s)	E (1/s)	μ (1/s)	$\overline{C}_0$ (g/s)
Downslope	1.80	1.36	924	0.0131	0.1380
Upslope	1.80	0.28	188	0.0131	0.0325

advection equation were applied to simulate overland flow and solute transport over the infiltrating slope under moving rainstorms and a spatially distributed and temporally decaying solute source. Since each set of solute transport processes was driven by three consecutive storms moving in the same direction (three downstream or three upstream moving storms), the model was first calibrated using the data of the first downstream and the first upstream moving storms. The results of the calibration were shown in Figures 5a and 6a. Values of the calibrated parameters are listed in Table 2. The initial transport rate $\overline{C}_0$ is calculated according to $\overline{C}_0 = QC_{m0}/\forall_{ML}$ (see Appendix B), where C_{m0} = mass of solute = 25 g. $\forall_{ML}$ = the total volume of the mixing zone = flume width $\times$ length $\times$ thickness of the mixing zone = $0.1 \times 2.0 \times D_m$. The mixing zone thickness D_m is taken as the maximum soil scouring depth observed in the flume. The peak discharge is used to calculate $\overline{C}_0$. The decay coefficient μ is determined based on the observed time needed to wash-off the salt applied. The fractional differential order F, dispersion coefficient K, and solute transfer parameter E are estimated by matching or fitting the mean travelling time, variance, and skewness of the simulated curves of solute transport rate with the corresponding measured one for the first upstream and downstream moving storms using the least-squares method. It can be seen from Table 2 that parameter F takes on a fractional value of 1.80 instead of the integer constant of 2, demonstrating the heterogeneity of the soil. The processes produced by downslope storms had greater values of the dispersion coefficient K, solute transfer parameter E, and initial transport rate $\overline{C}_0$ than those produced by upslope storms. The decay coefficient μ mainly depends on the property of the solute. Actually, μ represents the mean behavior of the solute decay in the mixing zone over some time period and hence it can be regarded as a constant. The rainfall intensity I at each grid point and at the time level was determined according to the fixed rainfall pattern in Figure 3 and velocity and direction of storms. The infiltration capacity of the soil was assumed to be $f = \eta I$ with coefficient η = 0.4$\sim$0.5 depending on the storm direction (downslope or upslope) because the soil was wetted to field capacity before rainfall was started. Thus the presumption that $f = \eta I$ is reasonable for this application but may not be so for many field conditions.

[35] For these calibrated parameter values, the numerical schemes described in the previous section yielded hydrographs, pollutographs, and concentration distributions, as plotted in Figures 4, 5b and 5c, 6b and 6c, and 7. In general, the predicted hydrographs fitted the measured data better than did pollutographs, and the downslope processes were simulated with a greater accuracy than the upslope processes. Both the downslope and the upslope processes exhibit long-tailed distributions but the downslope process displays a greater peak and a more rapid and concentrated flood process. However, the upslope rainfall induces a relatively flat runoff process with a smaller peak. Figures 4a and 4b show the hydrographs for the downslope and upslope moving rainfalls, respectively. Figures 5a–5c show pollutographs for three consecutive downslope moving rainfalls with the same time interval of 15 minutes. Owing to the decaying property, the salt was dissolved gradually and thus was not fully washed off, even after three runs. The peak transport rate nevertheless decreased significantly from the first to the third run. Figures 6a–6c give pollutographs for three consecutive upslope moving rainfalls with the same time interval of 15 minutes. It appears that the wash-off process of the solute is slow and takes a long time, as compared with that of downslope cases. The concentration distribution exhibits an inverse tendency to both hydrographs and pollutographs, as shown in Figure 7. At zero depth (no water) there was already solute on the land surface and thus the solute concentration would amount to a very high value. The peak flow discharge and transport rate of solute correspond to a minimum concentration. Then the concentration increased with time, because the pollutant (salt) is roughly exponentially dissolved and transferred from the active surface zone to runoff, while flow discharge decreased from a peak value to zero. Figure 8 clearly indicates the difference between the proposed fractional

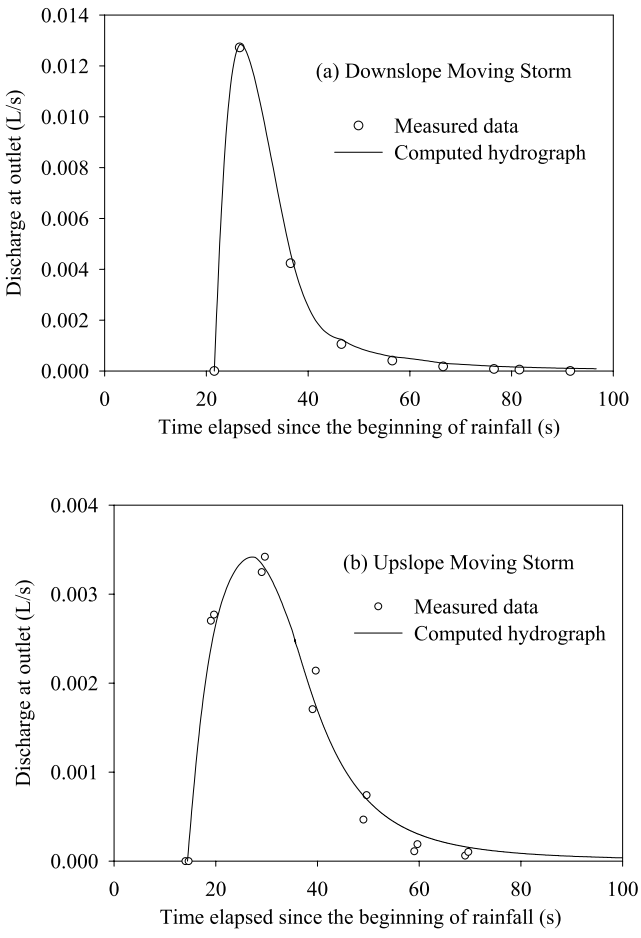

Figure 4. Hydrographs for downslope and upslope moving rainstorms; experimental data include two laboratory experiments.

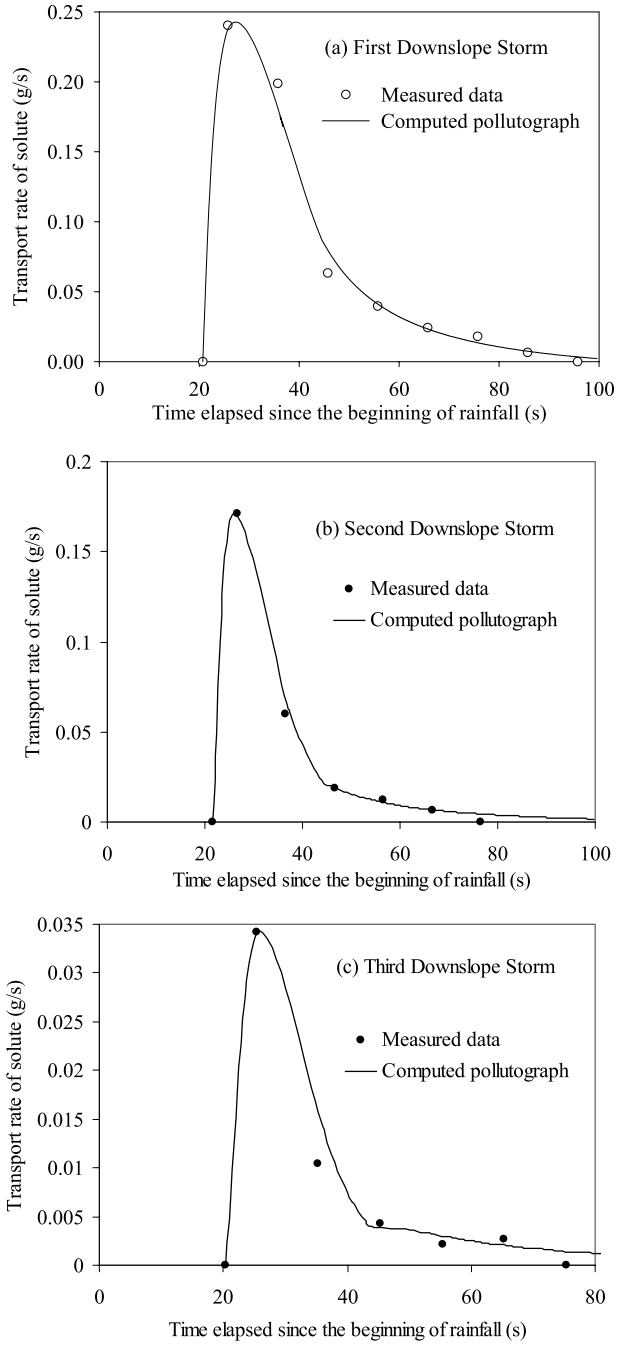

Figure 5. Influence of decaying source on pollutographs for three consecutive downslope moving rainstorms.

dispersion model (FADE) and the traditional integer-order ($F = 2$) model (ADE). The ADE model produces an earlier and greater peak than does the FADE model for the first storm and a smaller peak for latter storms, as shown in Figures 8a and 8b, respectively. This means that the ADE model predicts a faster flushing process of pollutants as compared to the FADE model. This is easily understood, since the fractional model takes account of the surface heterogeneity which yields a rougher surface as compared to the integer model. The heterogeneous surface may form hierarchical storage-release zones of solute, leading to the delayed transport process of the solute. Actually, the fractional model is a generalized overland solute transport model, including the integer-order model as a special case with $F = 2$. To assess the performance of the proposed fractional dispersion model, the following Nash-Sutcliffe coefficient of efficiency R^2, a statistical parameter recommended by the *ASCE Task Committee on Definition of Criteria for Evaluation of Watershed Models of the Watershed Management Committee* [1993] [*Nash and*

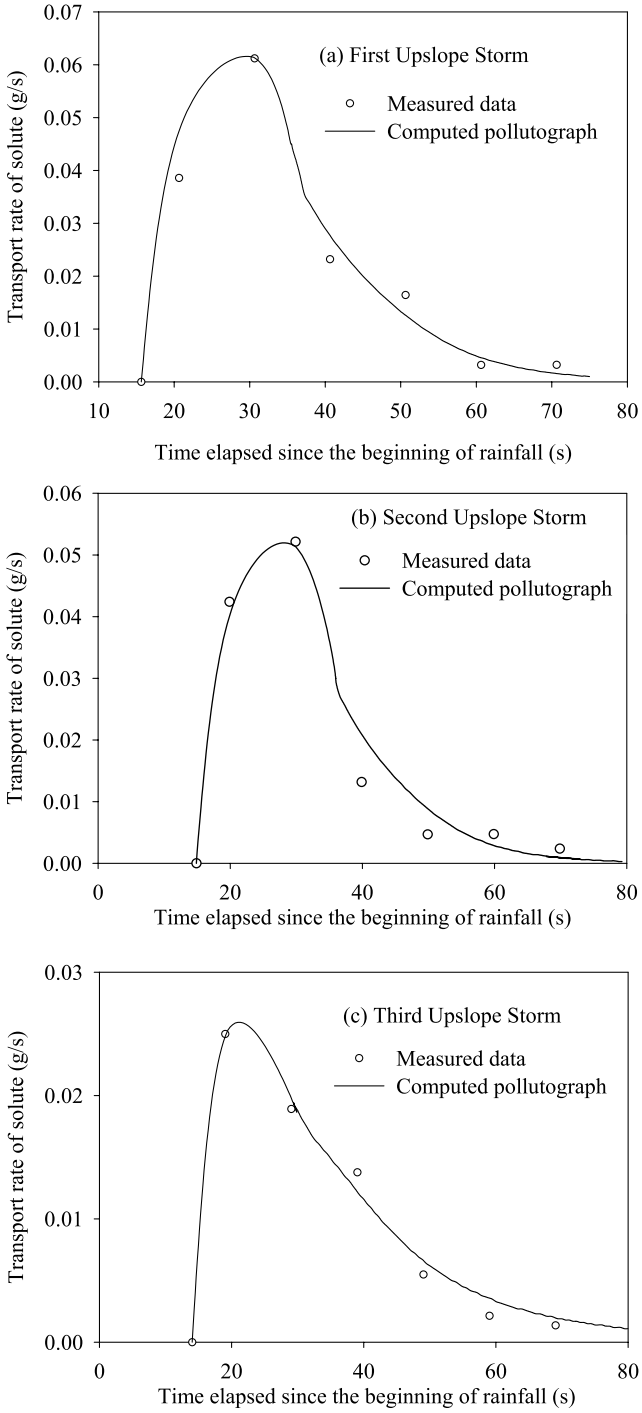

Figure 6. Influence of decaying source on pollutographs for three consecutive upslope moving rainstorms.

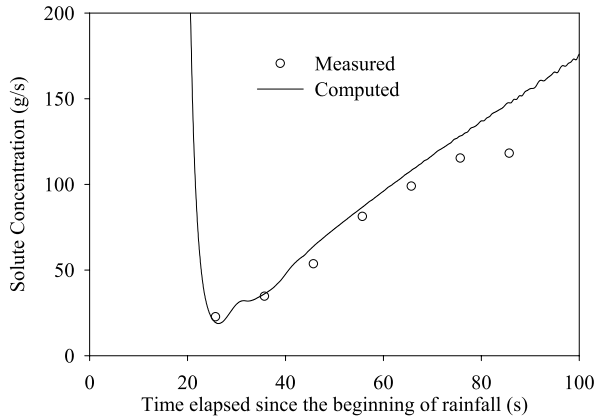

Figure 7. Concentration distribution for the first downslope moving rainstorm.

Sutcliffe, 1970], was used as a measure of relative error of the predictions:

$$R^2 = 1 - \left[\sum (V_m - V_p)^2\right] \Big/ \left[\sum (V_m - V_{avg})^2\right] \qquad (18)$$

where V_m = the measured value, V_p = the predicted value, V_{avg} = the average measured value. The R^2 values can vary from 0 to 1, with 1 indicating a perfect prediction, while a value of 0 represents a prediction no better than simply taking the average measured value. The calculated values of R^2 for the transport rate of solute are given in Table 3. This table indicates that downslope processes have higher R^2 values on average. In general, the values of R^2 in Table 3 are very close to 1.0 and so the FADE model performs very well in predicting the overland solute transport under decaying non-point source and moving rainstorms with varying intensity.

7. Summary and Conclusions

[36] Using the kinematic-wave overland flow equation and a fractional dispersion-advection equation, a process-oriented and physically-based model has been developed for solute transport over infiltrating hillslopes under moving rainstorms and a spatially distributed and temporally decaying pollutant source. Physically, the fractional dispersion term is used to describe the delayed release of pollutants or long-tailed dispersion process caused by surface and volume heterogeneities of the soil media. Mathematically, the fractional dispersion term is discretized by the F.3 central finite-difference scheme. The fractional dispersion-advection equation is numerically solved in the framework of a semi-Lagrangian approach. The kinematic-wave overland flow equation is solved efficiently using the Lax-Wendroff explicit scheme. The following conclusions are drawn from this study:

[37] 1. Hydrographs display a long-tailed distribution due to flow velocity variation with both the time and the distance. Solute transport exhibits a complex behavior. The pollutographs are characterized by a steep rising limb followed by a long stretched receding limb; whereas the solute concentration distribution features a rapidly receding limb followed by a long stretched rising limb.

[38] 2. Moving rainstorms have a significant influence on overland flow and solute transport. Downslope moving storms produce a much higher peak and a more concentrated distribution in both the hydrograph and the pollutograph than do the upslope moving storms, while upslope moving rainfall induces a relatively flat slope process with a smaller peak.

[39] 3. A decaying pollutant source leads to a slow and gradual solute transport and thus an increasing solute concentration, even if the flow decreases. This occurs if the flow duration is shorter than that of the source. It is possible that the pollutant cannot be flushed off even after several runoff processes, although the peak transport rate decreases significantly from the first run to the following runs.

[40] 4. Good agreements between simulated and measured dispersion characteristics demonstrate that the fractional dispersion model can accurately predict characteristics of overland flow and solute transport. The proposed fractional dispersion model includes the integer-order advection-dispersion equation as a special case. It can therefore be employed as a generalized model for overland flow and solute transport under realistic input conditions of

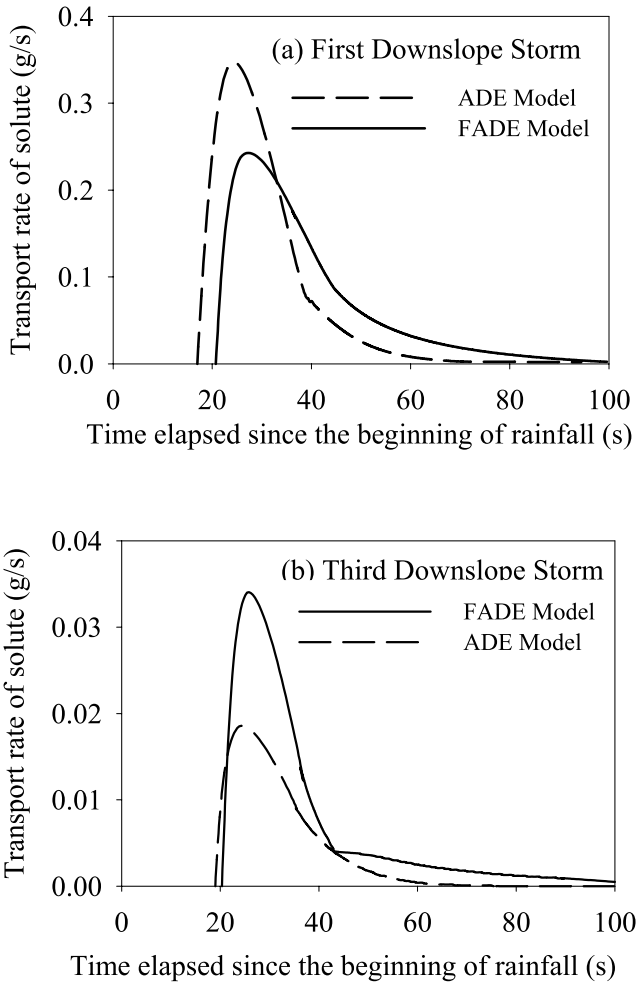

Figure 8. Comparison between the proposed fractional model and the traditional integer model.

Table 3. R^2 Values of Transport Rate of Solute

Runs	First Run	Second Run	Third Run
Downslope	0.9905	0.9982	0.9751
Upslope	0.9693	0.9706	0.9889

moving rainstorms with varying intensity and a spatially distributed and temporally decaying source.

Appendix A: Development of Numerical Solution for Fractional Dispersion-Transfer Equation

[41] The fractional derivative (dispersion) term in equation (14) can be discretized by the following F.3 central finite-difference scheme, recently presented by *Deng et al.* [2004]:

$$\frac{\partial^F \overline{C}}{\partial x^F} = \frac{\overline{C}^{\,n}_{j+1} - F\overline{C}^{\,n}_{j} + w_2^F \overline{C}^{\,n}_{j-1}}{\Delta x^F} + \frac{1}{\Delta x^F}\sum_{k=3}^{j+1} w_k^F \overline{C}^{\,n}_{j+1-k},$$
$$w_2^F = F(F-1)/2 \tag{A1a}$$

in which the binomial coefficient

$$w_k^F = \left(\frac{k-1-F}{k}\right) w_{k-1}^F, \quad w_0^F = 1,\ \mathrm{k} = 1,\ 2,\ 3,\ \ldots \tag{A1b}$$

where the series expression of the fractional derivative is divided into two parts because the binomial coefficients w_k^F decrease significantly when $k \geq 3$. When $F = 2$ the first part recovers the conventional central finite-difference scheme and the second part disappears. For dispersion processes in heterogeneous media the second part always exists. Furthermore, the second part is dependent on the distance scale j and time scale n. The larger the scales are, the smaller the coefficient w_k^F is. This means that the dispersion processes in natural media will gradually lose memory. The farther the current position from the grid point, the smaller the contribution from this point. The series can be hence regarded as a down-scaling system from $j = 0$ to $j = N$; $j = 0$ represents the largest scale and $j = N$ denotes the smallest scale. In theory, the series approximation approaches the fractional derivative when the distance scale tends to be infinite. Accordingly, the tail of a dispersion distribution should be infinitely long.

[42] It is desirable to render the solution of equation (14) unconditionally stable since the pure advection process is not subject to any stability limitation on the time step. To that end, equation (A1) is recast in the implicit form with a weighting factor λ as

$$\frac{\partial^F C}{\partial x^F} = \frac{1}{(\Delta x)^F}\left[\lambda\left(C_{j+1}^{n+2/3} - FC_j^{n+2/3} + w_2^F C_{j-1}^{n+2/3}\right) + (1-\lambda)\left(C_{j+1}^{n+1/3} - FC_j^{n+1/3} + w_2^F C_{j-1}^{n+1/3}\right)\right] + \frac{1}{\Delta x^F}\sum_{\mathrm{nt}=0}^{\mathrm{n}+1/3}\sum_{i=j+2}^{N} w_k^F\, C_i^{nt} \tag{A2}$$

in which $j = 1, 2, 3, \ldots N - 1$ (N = the total number of distance steps) and $k = i + 1 - j$; the weighting factor $0 \leq \lambda \leq 1$. It should be noted that in terms of the "long memory" of fractional derivatives the current status of a pollutant particle is related to its states at previous time levels. Substituting equation (A2) into equation (14) and utilizing the forward time scheme, equation (14) is discretized as:

$$\frac{\overline{C}_j^{\,n+2/3} - \overline{C}_j^{\,n+1/3}}{\Delta t/3} = \frac{K}{(\Delta x)^F}\left[\lambda\left(\overline{C}_{j+1}^{\,n+2/3} - F\overline{C}_j^{\,n+2/3} + w_2^F\overline{C}_{j-1}^{\,n+2/3}\right) + (1-\lambda)\left(\overline{C}_{j+1}^{\,n+1/3} - F\overline{C}_j^{\,n+1/3} + w_2^F\,\overline{C}_{j-1}^{\,n+1/3}\right)\right] + \frac{K}{\Delta x^F}\sum_{\mathrm{nt}=0}^{\mathrm{n}+1/3}\sum_{i=j+2}^{N} w_k^F\,\overline{C}_i^{\,nt} + E\left(\frac{\overline{C}_{sj}^{\,n+2/3} + \overline{C}_{sj}^{\,n+1/3}}{2} - \frac{\overline{C}_j^{\,n+2/3} + \overline{C}_j^{\,n+1/3}}{2}\right) \tag{A3}$$

Equation (4e) is discretized as

$$\overline{C}_{sj}^{\,n+2/3} = \overline{C}_0 \exp[-\mu(n+2/3)\Delta t] = \overline{C}_{sj}^{\,n+1/3}\exp[-\mu\Delta t/3] \tag{A4}$$

Substituting equation (A4) into equation (A3) and rearranging equation (A3) so that all the known quantities appear on the RHS and all the unknown quantities appear on the LHS yields:

$$-w_2^F\varphi\lambda\overline{C}_{j-1}^{\,n+2/3} + (1+\beta+\varphi\lambda F)\overline{C}_j^{\,n+2/3} - \varphi\lambda\overline{C}_{j+1}^{\,n+2/3} = \varphi(1-\lambda)\overline{C}_{j+1}^{\,n+1/3} + [1-\beta-F\varphi(1-\lambda)]\overline{C}_j^{\,n+1/3} + w_2^F\varphi(1-\lambda)\overline{C}_{j-1}^{\,n+1/3} + \gamma\beta\overline{C}_{sj}^{\,n+1/3} + \varphi\sum_{\mathrm{nt}=0}^{\mathrm{n}+1/3}\sum_{i=j+2}^{N} w_k^F\overline{C}_i^{\,nt} \tag{A5}$$

in which

$$\varphi = \frac{K\Delta t}{3(\Delta x)^F}, \quad \beta = \frac{E\Delta t}{6}, \quad \gamma = 1 + e^{-\mu\Delta t/3} \tag{A6}$$

As $\overline{C}_{s\,\mathrm{j}}^{\,\mathrm{n}+1/3}$ is unknown, it is assumed that $\overline{C}_{s\,\mathrm{j}}^{\,\mathrm{n}+1/3} = \overline{C}_{s\,\mathrm{j}}^{\,\mathrm{n}}$. Then all the quantities appearing on the RHS of equation (A5) are known. Grouping the terms of equation (A5) yields equation (15) in the main text.

Appendix B: Derivation of the Equation of Solute Concentration in the Mixing Layer

[43] Based on the mass conservation principle and the Reynolds transport theorem, the integral form of the continuity equation for solute transport from the mixing zone to the overlying runoff can be expressed as

$$\frac{d}{dt}\int_{MZ}\rho d\forall + \int_{SS}\rho\vec{V}\cdot d\vec{A} = 0 \tag{B1}$$

where ρ is the density of the solute, $\forall$ represents the volume of solute in the mixing zone (MZ) or the control volume, $\vec{V}$ denotes the velocity of solute transport across the control surface or the soil surface (SS) with an area $\vec{A}$. As the rainfall-induced overland solute transport is a wash-off process of the solute from the mixing zone to the runoff, the only transport of solute is therefore from the mixing layer to the overland flow. Thus equation (B1) can be rewritten as

$$\frac{d(C_s\cdot\forall_{ML})}{dt} + \int_{SS}\rho\mathrm{VdA} = 0 \tag{B2}$$

where C_s is the concentration of the solute in the mixing zone [M/L^3], $\forall_{ML}$ is the total volume of the mixing zone [L^3]. The integral term in equation (B2) stands for the washoff mass of solute across the soil surface per unit time from the mixing zone to runoff. Due to the difficulty involved in the determination of the upward velocity V of solute transport across the soil surface, the integral term is approximated by $C_s \cdot \mu\forall_{ML}$, where μ is a coefficient depending on the properties of soil and the solute and carrying a dimension of [T^{-1}]. μ can be estimated using experimental data. Let $C_m = C_s \cdot \forall_{ML}$. Then, equation (B2) can be recast as

$$\frac{dC_m}{dt} + \mu C_m = 0 \quad \text{or} \quad \int_{C_{m0}}^{C_m} \frac{dC_m}{C_m} = -\mu \int_0^t dt \tag{B3}$$

in which C_{m0} and C_m are the solute mass stored or remaining in the mixing zone at the time of $t = 0$ and $t = t$. Integration of equation (B3) yields

$$\ln\left(\frac{C_m}{C_{m0}}\right) = -\mu t \quad \text{or} \quad C_m = C_{m0}\exp(-\mu t) \tag{B4}$$

Dividing both sides of equation (B4) by $\forall_{ML}$ and multiplying by the flow discharge Q_f results in equation (4e) in the main text, where $\overline{C}_s = QC_s$ and $\overline{C}_0 = QC_{m0}/\forall_{ML}$.

References

Abbott, M. B., and J. C. Refsgaard (1996), *Distributed Hydrological Modelling*, pp. 121–141, Springer, New York.

ASCE Task Committee on Definition of Criteria for Evaluation of Watershed Models of the Watershed Management Committee (1993), Criteria for evaluation of watershed models, *J. Irrig. Drain. Eng.*, *119*(3), 429–443.

Benson, D. A., S. W. Wheatcraft, and M. M. Meerschaert (2000a), The fractional-order governing equation of Lévy motion, *Water Resour. Res.*, *36*(6), 1413–1423.

Benson, D. A., S. W. Wheatcraft, and M. M. Meerschaert (2000b), Application of a fractional advection-dispersion equation, *Water Resour. Res.*, *36*(6), 1403–1412.

Berkowitz, B., J. Klafter, R. Metzler, and H. Scher (2002), Physical pictures of transport in heterogeneous media: Advection-dispersion, random-walk, and fractional derivative formulations, *Water Resour. Res.*, *38*(10), 1191, doi:10.1029/2001WR001030.

Chaves, A. S. (1998), A fractional diffusion equation to describe Lévy flights, *Phys. Lett. A*, *239*(1–2), 13–16.

de Lima, J. L. M. P., V. P. Singh, and M. I. P. de Lima (2002), The influence of storm movement on water erosion: Storm speed and direction effects, *CATENA*, *715*, 1–18.

Deng, Z.-Q., V. P. Singh, and L. Bengtsson (2004), Numerical solution of fractional advection-dispersion equation, *J. Hydraul. Eng.*, *130*(5), 422–431.

Fischer, H. B., E. J. List, R. C. Y. Koh, J. Imberger, and N. H. Brooks (1979), *Mixing in Inland and Coastal Waters*, pp. 30–138, Elsevier, New York.

Govindaraju, R. S. (1996), Modeling overland flow contamination by chemicals mixed in shallow soil horizons under variable source area hydrology, *Water Resour. Res.*, *32*(3), 753–758.

Haggerty, R., S. M. Wondzell, and M. A. Johnson (2002), Power-law residence time distribution in the hyporheic zone of a 2nd-order mountain stream, *Geophys. Res. Lett.*, *29*(13), 1640, doi:10.1029/2002GL014743.

Harvey, J. W., B. J. Wagner, and K. E. Bencala (1996), Evaluating the reliability of the stream tracer approach to characterize stream-subsurface water exchange, *Water Resour. Res.*, *32*(8), 2441–2451.

Holly, F. M., and A. Preissmann (1977), Accurate calculation of transport in two-dimensions, *J. Hydraul. Div.*, *103*(11), 1259–1277.

Holly, F. M., and J.-D. Usseglio-Polatera (1984), Accurate two-dimensional simulation of advective-diffusive-reactive transport, *J. Hydraul. Eng.*, *127*(9), 728–737.

Hubbard, R. K., R. G. Williams, and M. D. Erdman (1989a), Chemical transport from coastal plain soils under simulated rainfall: I. Surface runoff, percolation, nitrate, and phosphate movement, *Trans. ASAE*, *32*(4), 1239–1249.

Hubbard, R. K., R. G. Williams, M. D. Erdman, and L. R. Marti (1989b), Chemical transport from coastal plain soils under simulated rainfall: II. Movement of cyanazine, sulfometuron-methy1, and bromide, *Trans. ASAE*, *32*(4), 1250–1257.

Hunt, B. (1999), Dispersion model for mountain streams, *J. Hydraul. Eng.*, *125*(2), 99–105.

Karpik, S. R., and S. R. Crockett (1997), Semi-Lagrangian algorithm for two-dimensional advection-diffusion equation on curvilinear coordinate meshes, *J. Hydraul. Eng.*, *123*(5), 389–401.

McCutcheon, S. C. (1989), *Water Quality Modeling*, vol. 1, *Transport and Surface Exchange in Rivers*, pp. 27–71, CRC Press, Boca Raton, Fla.

Meerschaert, M. M., D. A. Benson, and B. Bäumer (1999), Multidimensional advection and fractional dispersion, *Phys. Rev. E*, *59*(5), 5026–5028.

Nash, J. E., and J. V. Sutcliffe (1970), River flow forecasting through conceptual models, Part 1: A discussion of principles, *J. Hydrol.*, *10*(3), 282–290.

Oldham, K. B., and J. Spanier (1974), *The Fractional Calculus*, Elsevier, New York.

Podlubny, I. (1999), *Fractional Differential Equations*, pp. 41–242, Elsevier, New York.

Press, W. H., B. P. Flannery, S. A. Teukolsky, and W. T. Vetterling (1988), *Numerical Recipes*, pp. 77–101, 615–666, 704–708, Cambridge Univ. Press, New York.

Schumer, R., D. A. Benson, M. M. Meerschaert, and B. Baeumer (2003), Fractal mobile/immobile solute transport, *Water Resour. Res.*, *39*(10), 1296, doi:10.1029/2003WR002141.

Schumer, S., D. A. Benson, M. M. Meerschaert, and S. W. Wheatcraft (2001), Eulerian derivation of the fractional advection-dispersion equation, *J. Contam. Hydrol.*, *48*(1/2), 69–88.

Singh, V. P. (1996), *Kinematic Wave Modeling in Water Resources: Surface-Water Hydrology*, pp. 676–940, John Wiley, Hoboken, N. J.

Singh, V. P. (1997), *Kinematic Wave Modeling in Water Resources: Environmental Hydrology*, pp. 897–940, John Wiley, Hoboken, N. J.

Singh, V. P. (2002), Kinematic wave solution for pollutant transport over an infiltrating plane with finite-period mixing and mixing zone, *Hydrol. Processes*, *16*(12), 2441–2477.

Tuma, J. J., and R. A. Walsh (1998), *Engineering Mathematics Handbook*, McGraw-Hill, New York.

van Genuchten, M. T., and P. J. Wierenga (1976), Mass transfer studies in sorbing porous media 1, Analytical solutions, *Soil Sci. Soc. Am. J.*, *40*, 473–480.

Wallach, R., G. Grigorin, and J. Rivlin (2001), A comprehensive mathematical model for transport of soil-dissolved chemicals by overland flow, *J. Hydrol.*, *247*, 85–99.

Wan, Z.-H., and S.-L. Huang (1999), Effect of sediment on pollutant transport-transformation, in *Environmental Hydraulics*, edited by J. H. W. Lee, A. W. Jayawardena, and Z. Y. Wang, pp. 713–722, Balkema, Rotterdam.

Wheatcraft, S. W., and S. Tyler (1988), An explanation of scale dependent dispersivity in heterogeneous aquifers using concepts of fractal geometry, *Water Resour. Res.*, *24*, 566–578.

Woolhiser, D. A. (1975), Simulation of unsteady overland flow, in *Unsteady Flow in Open Channels*, vol. 2, edited by K. Mahmood and V. Yevjevich, pp. 485–508, Water Resour. Publ., Fort Collins, Colo.

Wörman, A., A. I. Packman, H. Johansson, and K. Jonsson (2002), Effect of flow-induced exchange in hyporheic zones on longitudinal transport of solutes in streams and rivers, *Water Resour. Res.*, *38*(1), 1001, doi:10.1029/2001WR000769.

Zhou, L., and H. M. Selim (2003), Application of the fractional advection-dispersion equation in porous media, *Soil Sci. Soc. Am. J.*, *67*, 1079–1084.

J. L. M. P. de Lima, IMAR – Institute of Marine Research, Coimbra Interdisciplinary Centre; Department of Civil Engineering, Faculty of Science and Technology, Polo 2 – University of Coimbra, 3030-290 Coimbra, Portugal.

M. I. P. de Lima, IMAR – Institute of Marine Research, Coimbra Interdisciplinary Centre; Department of Forestry, Agrarian Technical School of Coimbra, Polytechnic Institute of Coimbra, Bencanta, 3040-316 Coimbra, Portugal.

Z.-Q. Deng and V. P. Singh, Department of Civil and Environmental Engineering, Louisiana State University, Baton Rouge, LA 70803-6405, USA. (zdeng@lsu.edu)